glucose concentration in the medium was increased from 2.8 to 20 mM, the corresponding increases in both $[ATP]_m$ (Fig. 10A) and $[ATP]_c$ (Fig. 10C) were similar to the increases in $[ATP]_m$ and $[ATP]_c$ observed in islets cultured with normal Ca^{2+}-containing medium (Fig. 10B, D). To test the requirement of the intracellular Ca^{2+} pool, BAPTA-AM, a chelator of intracellular Ca^{2+}, was added. Pretreatment of islets with BAPTA-AM almost completely suppressed the increases in both $[ATP]_m$ (Fig. 10E) and $[ATP]_c$ (Fig. 10F) after glucose stimulation. Moreover, treatment of islets cultured in low-glucose medium with BAPTA-AM decreased $[ATP]_m$ (Fig. 10G). These data indicate that intracellular Ca^{2+}, rather than extracellular Ca^{2+}, is required for glucose-induced ATP elevation and for maintaining basal intracellular ATP levels.

DISCUSSION

In this paper, we fluorescently imaged the dynamics of both $[ATP]_c$ and $[Ca^{2+}]_c$ in single isolated mouse pancreatic islets, using a genetically encoded FRET-based ATP biosensor, GO-ATeam1, and a fluorescent Ca^{2+} dye, fura-2. We demonstrated that stimulation of islets with glucose, MP, or leucine/glutamine all induced rapid increase of $[ATP]_c$, followed by that of $[Ca^{2+}]_c$. These results are almost consistent with a recent report that glucose-induced ATP/ADP ratio elevation is followed by depolarization of plasma membrane and $[Ca^{2+}]_c$ rise (14). Pharmacological inhibition of energy metabolism blocked increases of both $[ATP]_c$ and $[Ca^{2+}]_c$ in all situations, indicating that increase in ATP production or energy metabolism is the fundamental mechanism that triggers the $[Ca^{2+}]_c$ burst in the initial phase of GSIS, as well as both MP-stimulated and leucine/glutamine-stimulated insulin secretion.

Oscillation of $[Ca^{2+}]_c$ in the second phase of GSIS is a typical feature of islets or β-cells (6, 7, 8) and is assumed to be required for pulsatile insulin secretions (6). For the generation of such Ca^{2+} oscillation, oscillatory activities of the K_{ATP} channel have been implicated by the observation that islets of Kir6.2$^{-/-}$ mice exhibited high non-oscillatory intracellular Ca^{2+} levels after glucose or tolbutamide stimulation (36). To explain the oscillatory activities of the K_{ATP} channel, it has long been believed that intracellular ATP levels also oscillate during the insulin secretion. In contrast to this generally believed view, however, we did not observe any significant oscillations of $[ATP]_c$ in isolated mouse pancreatic islets and in single islet cells during GSIS. Consistent with this, it has been also shown that mitochondrial bioenergetic activities do not oscillate in glucose- or pyruvate-stimulated INS-1 832/13 cells (29). Conversely, a recent study has reported that $[Ca^{2+}]$ oscillation in glucose-stimulated isolated mouse islet cells induces small oscillation of ATP levels near the plasma membrane ($[ATP]_{pm}$) (15). This small local oscillation of ATP level was, however, suggested to be a result of enhanced local ATP consumption by increased Ca^{2+} (15). It is notable that GO-ATeam1 is able to detect $[ATP]_c$ changes of approximately 1 mM in insulin-secreting cells (Fig. 1). Thus, the amplitude of $[ATP]_c$ oscillation would be much less than 1 mM, even if it exists. Given that mitochondria supply large amount of ATP to bulk cytosolic space, it is not surprising that the bulk cytosolic ATP levels inside pancreatic β-cells are almost constant in the second phase of GSIS even when $[ATP]_{pm}$ oscillates.

Alternation of FRET signal of GO-ATeam1 by both glucose-stimulation and metabolic

inhibitors indicates that $[ATP]_c$ of pancreatic β-cell is within the dynamic range of the biosensor, which is about 2-20 mM (Fig. 1 and ref. 17). Apparently, this high concentration of cytosolic ATP could not regulate the K_{ATP} channel in β-cells, since the channel is blocked by the Mg^{2+}-unbound form of ATP with an approximate K_i value of 10 μM (3, 37). However, Mg^{2+}-unbound form of ATP exists at quite low levels inside cells, because of the high affinity of ATP to Mg^{2+}. Indeed, the most of K_{ATP} channel activity is blocked by physiological ATP levels in the presence of Mg^{2+} (2). Only slight increases of ATP levels, thus, could be sufficient for switching off the activity of the K_{ATP} channel.

Our data, presented in this study, collectively supported the possibility that sustained high levels of $[ATP]_c$ via energy metabolism, rather than its oscillation, are required for maintaining the oscillation of $[Ca^{2+}]_c$ of pancreatic β-cells. However, we could not currently exclude the possibility that slight oscillation of free ATP levels is causative for the production of oscillatory K_{ATP} channel activities, and thus further examinations are required to fully answer the question as to how oscillatory K_{ATP} channel activities are created. Alternation of energy metabolism will also affect intracellular ADP level. It was reported that Mg^{2+}-bound ADP antagonizes the ATP binding of K_{ATP} channels (38). Thus, it is also possible that not only ATP levels but also ADP levels (or ATP/ADP ratio) are involved in the regulation of K_{ATP} channels in GSIS. However, because no technique to specifically monitor ADP in living culture cells is currently available, it is quite difficult to know ADP dynamics in islet. If a genetically encoded biosensor for ADP is established, it will contribute to more detailed understanding of the mechanism of opening and closing of K_{ATP} channels.

Another notable finding is that the uncoupling of mitochondria or reduction of medium glucose levels immediately arrested oscillation of $[Ca^{2+}]_c$ with a slight drop in $[ATP]_c$ (Fig. 9A and B), suggesting that β-cells are able to sense a small decrease in energy supply, namely a blood glucose levels, probably sensing a slight reduction in $[ATP]_c$. This system would be suitable for maintaining the energy homeostasis of the whole body. If complete depletion of $[ATP]_c$ to the basal level were required to halt oscillation of $[Ca^{2+}]_c$, a significant amount of insulin would continue to be secreted even at low blood glucose levels, leading to hypoglycemia.

The dysfunction of β-cells is one of the hallmarks of type 2 diabetes, in which insulin secretion is attenuated even after glucose stimulation (39-43). According to our imaging data, maintaining elevated $[ATP]_c$ must be necessary for insulin secretion, so it is conceivable that the dynamics of $[ATP]_c$ is impaired in islets of diabetic mouse models or human patients.

REFERENCES

1. Ashcroft, F. M., Proks, P., Smith, P. A., Ammälä, C., Bokvist, K., and Rorsman, P. (1994) Stimulus-secretion coupling in pancreatic β-cells. *J. Cell. Biochem.* 55, suppl, 54-65
2. Ashcroft, F. M. (2000) ATP-sensitive potassium channelopathies: focus on insulin secretion. *J. Clin. Invest.* 115, 2047-2058
3. Inagaki, N., Gonoi, T., Clement, J. P. 4th., Namba, N., Inazawa, J., Gonzalez, G., Aguilar-Bryan, L., Seino, S., and Bryan, J. (1995) Reconstitution of I_{KATP}: an inward rectifier subunit plus the sulfonylurea receptor. *Science* 270, 1166-1170
4. Inagaki, N., and Seino, S. (1998) ATP-sensitive potassium channels: structures, functions and pathophysiology. *Jpn. J. Physiol.* 48, 397-412
5. Miki, T., Tashiro, F., Iwanaga, T., Nagashima, K., Yoshitomi, H., Aihara, H., Nitta, Y., Gonoi, T., Inagaki, N., Miyazaki, J., and Seino, S. (1997) Abnormalities of pancreatic islets by targeted expression of a dominant-negative K_{ATP} channel. *Proc. Natl. Acad. Sci. USA* 94, 11969-11973
6. Gilon, P., Shepherd, R. M., and Henquin, J. C. (1993) Oscillations of secretion driven by oscillations of cytoplasmic Ca^{2+} as evidenced in single pancreatic islets. *J. Biol. Chem.* 268, 22265-22268
7. Gilon, P., and Henquin, J. C. (1992) Influence of membrane potential changes on cytoplasmic Ca^{2+} concentration in an electrically excitable cell, the insulin-secreting pancreatic B-cell. *J. Biol. Chem.* 267, 20713-20720
8. Tengholm, A., and Gylfe, E. (2009) Oscillatory control of insulin secretion. *Mol. Cell. Endocri.* 297, 58-72
9. Ghosh, A., Ronner, P., Cheong, E., Khalid, P., and Matschinky, F. M. (1991) The role of ATP and free ADP in metabolic coupling during fuel-stimulated insulin release from islet β-cells in the isolated perfused rat pancreas. *J. Biol. Chem.* 266, 22887-22892
10. Lorenz, M. A., El Azzouny, M. A., Kennedy, R. T., and Burant, C. F. (2013) Metabolome response to glucose in the β-cell line INS-1 832/13. *J. Biol. Chem.* 288, 10923-10935
11. Bo Hellman, M. D., Lars-Ake Idahl, M. K., and Ake Danielsson, M. K. (1969) Adenosine triphosphate levels of mammalian pancreatic B cells after stimulation with glucose and hypoglycemic sulfonylureas. *Diabetes* 18, 509-516
12. Ashcroft, S. J. H., Weerasinghe, L. C. C., and Randle, P. J. (1973) Interrelationship of islet metabolism, adenosine triphosphate content and insulin release. *Biochem. J.* 132, 223-231

13. Düfer, M., Krippeit-Drews, P., Buntinas, L., Slemen, D., and Drews, G. (2002) Methyl pyruvate stimulates pancreatic β-cells by direct effect on K_{ATP} channels, and not as a mitochondrial substrate. *Biochem. J.* 368, 817-825
14. Tarasov, A. I., Semplici, F., Ravier, M. A., Bellomo, E. A., Pullen, T. J., Gilon, P., Sekler, I., Rizzuto, R., and Rutter, G. A. (2012) The mitochondrial Ca^{2+} uniporter MCU is essential for glucose-induced ATP increases in pancreatic β-cells. *PLoS ONE* 7, e39722
15. Li, J., Shuai, H. Y., Gylfe, E., and Tengholm, A. (2013) Oscillations of sub-membrane ATP in glucose-stimulated beta cells depend on negative feedback from Ca^{2+}. *Diabetologia* 56, 1577-1586
16. Imamura, H., Nhat, K. P., Togawa, H., Saito, K., Iino, R., Kato-Yamada, Y., Nagai, T., and Noji, H. (2009) Visualization of ATP levels inside single living cells with fluorescence resonance energy transfer-based genetically encoded indicators. *Proc. Natl. Acad. Sci. USA* 106, 15651-15656
17. Nakano, M., Imamura, H., Nagai, T., and Noji, H. (2011) Ca^{2+} regulation of mitochondrial ATP synthesis visualized at the single cell level. *ACS. Chem. Biol.* 6, 709-715
18. Miyazaki, J., Araki, K., Yamamoto, E., Ikegami, H., Asano, T., Shibasaki, Y., Oka, Y., and Yamamura, K. (1990) Establishment of a pancreatic β cell line that retains glucose-inducible insulin secretion: special reference to expression of glucose transporter isoform. *Endocrinology* 127, 126-132
19. Terasawa, S., Fukuoka, H., Inoue, Y., Sagawa, T., Takahashi, H., and Ishijima, A. (2011) Coordinated reversal of flagellar motors on a single *Escherichia coli* cell. *Biophys. J.* 100, 2193-2200
20. Pullen, T. J., da Silva Xavier, G., Kelsey, G., and Rutter, G. A. (2011) MiR-29a and miR-29b contribute to pancreatic β-cell-specific silencing of monocarboxylate transporter 1 (Mct1). *Mol. Cel. Biol.* 31, 3182-3194
21. Mertz, R. J., Worley, J. F., Spencer, B., Johnson, J. H., and Dukes, I. D. (1996) Activation of stimulus-secretion coupling in pancreatic β-cells by specific products of glucose metabolism. *J. Biol. Chem.* 271, 4838-4845
22. Zawalich, W. S., and Zawalich, K. C. (1997) Influence of pyruvic acid methyl ester on rat pancreatic islets. *J. Biol. Chem.* 272, 3527-3531
23. Lembert, N., Joes, H. C., Idahl, L. A., Ammon, H. P., and Wahl, M. A. (2001) Methyl pyruvate initiates membrane depolarization and insulin release by metabolic factors other than ATP. *Biochem. J.* 354, 345-350

24. Stanley, C. A., Lieu, Y. K., Hsu, B. Y., Burlina, A. B., Greenberg, C. R., Hopwood, N, J., Perlman, K., Rich, B. H., Zammarchi, E., and Poncz, M. (1998) Hyperinsulinism and hyperammonemia in infants with regulatory mutations of the glutamate dehydrogenase gene. *N. Engl. J. Med.* 338, 1352-1357
25. Carobbio, S., Frigerio, F., Rubi, B., Vetterli, L., Bloksgaard, M., Gjinoxci, A., Pournourmohammadi, S., Herrera, P. L., Reith, W., Mandrup, S., and Maechler, P. (2009) Deletion of glutamate dehydrogenase in β-cells abolishes part of the insulin secretory response not required for glucose homeostasis. *J. Biol. Chem.* 284, 921-929
26. Li, C., Najafi, H., Daikhin, Y., Nissim, I. B., Collins, H. W., Yudkoff, M., Matschinsky, F. M., and Stanley, C. A. (2003) Regulation of leucine-stimulated insulin secretion and glutamine metabolism in isolated rat islets. *J. Biol. Chem.* 278, 2853-2858
27. Fahien, L. A., and Macdonald, M. J. (2011) The complex mechanism of glutamate dehydrogenase in insulin secretion. *Diabetes* 60, 2450-2454
28. Ainscow, E. K., and Rutter, G. A. (2002) Glucose-stimulated oscillations in free cytosolic ATP concentration imaged in single islet β-cells: evidence for a Ca^{2+}-dependent mechanism. *Diabetes* 51, S162-S170
29. Goehring, I., Gerencser, A. A., Schmidt, S., Brand, M. D., Mulder, H., and Nicholls, D. G. (2012) Plasma membrane potential oscillations in insulin secreting Ins-1 823/13 cells do not require glycolysis and are not initiated by fluctuations in mitochondrial bioenergetics. *J. Biol. Chem.* 287, 15706-15717
30. McCormack, J. G., Halestrap, A. P., and Denton, R. M. (1990) Role of calcium ions in regulation of mammalian intramitochondrial metabolism. *Physiol. Rev.* 70, 391-425
31. Wiederkehr, A., Szanda, G., Akhmedov, D., Mataki, C., Heizmann, C. W., Schoonjans, K., Pozzan, T., Spät, A., and Wollheim, C. B. (2011) Mitochondrial matrix calcium is an activating signal for hormone secretion. *Cell. Metab.* 13, 601-611
32. Stefani, D. D., Raffaello, A., Teardo, E., Szabo, I., and Rizzuto, R. (2011) A forty-kilodalton protein of inner membrane is the mitochondrial calcium uniporter. *Nature* 476, 336-340
33. Baughman, J. M., Perocchi, F., Girgis, H. S., Plovanich, M., Belcher-Timme, C. A., Sancak, Y., Bao, X. R., Strittmatter, L., Goldberger, O., Bogorad, R. L., Koteliansky, V., and Mootha, V. K. (2011) Integrative genomics identifies MCU as an essential component of mitochondrial calcium uniporter. *Nature* 476:341-345
34. Jiang, D., Zhao, L., and Clapham, D. E. (2009) Genome-wide RNAi screen identified

Letm1 as a mitochondrial Ca^{2+}/H^{+} antiporter. *Science* 326, 144-147

35. Trenker, M., Malli, R., Fertschai, I., Levak-Frank, S., and Graier, W. F. (2007) Uncoupling protein 2 and 3 are fundamental for mitochondrial Ca^{2+} uniport. *Nat. Cell. Biol.* 9, 445-452
36. Miki, T., Nagashima, K., Tashiro, F., Kotake, K., Yoshitomi, H., Tamamoto, A., Gonoi, T., Iwanaga, T., Miyazaki, J., and Seino, S. (1998) Defective insulin secretion and enhanced insulin action in K_{ATP} channel-deficient mice. *Proc. Natl. Acad. Sci. USA* 95, 10402-10406
37. Gribble, F. M., Tucker, S. J., Haug, T., and Ashcroft, F. M. (1998) MgATP activates the β cell K_{ATP} channel by interaction with its SUR1 subunit. *Proc. Natl. Acad. Sci. USA* 95, 7185-7190
38. Ueda, K., Inagaki, N., and Seino, S. (1997) MgADP antagonism to Mg^{2+}-independent ATP binding of the sulfonylurea receptor SUR1. *J. Biol. Chem.* 272, 22983-22986
39. Pratley, R. E., and Weyer, C. (2001) The role of impaired early insulin secretion in the pathogenesis of Type II diabetes mellitus. *Diabetaologia* 44, 929-945
40. Anello, M., Lupi, R., Spampinato, D., Piro, S., Masini, M., Boggi, U., Del Prato, S., Rabuazzo, A. M., Purrello, F., and Marchetti, P. (2005) Functional and morphological alterations of mitochondria in pancreatic beta cells from Type 2 diabetic patients. *Diabetologia* 48, 282-289
41. Maechler, P., and Wollheim, C. B. (2001) Mitochondrial function in normal and diabetic β-cells. *Nature* 414, 807-812
42. Yoshihara, E., Fujimoto, S., Inagaki, N., Okawa, K., Masaki, S., Yodoi, J., and Masutani, H. (2010) Disruption of TBP-2 ameliorates insulin sensitivity and secretion without affecting obesity. *Nat. Commun.* 1, 127
43. Ohtsubo, K., Chen, M. Z., Olefsky, J. M., and Marth, J. D. (2011) Pathway to diabetes through attenuation of pancreatic beta cell glycosylation and glucose transport. *Nat. Med.* 17, 1067-1076

Acknowledgements - This work was supported in part by Grants-in-Aid for Scientific Research 22590977 (to K.N.) and by Platform for Dynamic Approaches to Living System (to T.T and H.I.) from the Ministry of Education, Culture, Sports, Science, and Technology in Japan, as well as by Precursory Research for Embryonic Science (to H.I.) from the Japan Science and Technology Agency. We greatly appreciate the gifts of MIN6 cells from Dr. Jun-ichi Miyazaki (Osaka University). We also thank Dr. James Hejna (Kyoto University) for his critical assessment of this manuscript.

FIGURE LEGENDS

FIGURE 1. Validation of GO-ATeam in insulin-secreting cells. Time course of the fluorescence emission ratio (OFP/GFP) in permeabilized MIN6 cells expressing GO-ATeam1 biosensors in the cytosol. (A) After permeabilization, cells were perfused with intracellular-like medium including different concentrations (2–10 mM) of MgATP (n = 9). (B) After permeabilization, cells were alternately perfused with intracellular-like medium including 7 or 8 mM MgATP (n = 10). (C) Average time course of the fluorescence emission ratio (OFP/GFP) of MIN6 cells expressing GO-ATeam1 biosensors in the cytosol. OFP/GFP ratios were monitored when medium glucose was increased from 2.8 to 25 mM (n = 22). Cells that did not exhibit clear increases in response to changing glucose levels were excluded from the data analysis. Error bars indicate the standard deviation (SD).

FIGURE 2. Glucose stimulation induces a rapid increase in cytosolic and mitochondrial ATP levels in single isolated mouse islets. (A, B) Time course of the fluorescence emission ratio (OFP/GFP) of isolated islets expressing GO-ATeam biosensors in the cytosol. OFP/GFP ratios of GO-ATeam1 (A) or GO-ATeam3 (B) were monitored when medium glucose was increased from 2.8 to 25 mM (n = 13 and 4, respectively). (C) Time course of the fluorescence emission ratio (YFP/CFP) of isolated islets expressing ATeam1.03 (AT1.03) biosensors in the cytosol. YFP/CFP ratios were monitored when medium glucose was increased from 2.8 to 25 mM (n = 4). (D) The average time course of OFP/GFP ratios of isolated islets expressing GO-ATeam1. OFP/GFP ratios were monitored in the same islets when glucose was increased from 2.8 to 8.3, 16.7, and 25 mM (n = 10). Error bars indicate standard deviation (SD). (E) The amplitudes of OFP/GFP ratio changes were quantified in various glucose conditions shown in (D). Error bars indicate the standard deviation (SD) and asterisks indicate significant differences. $*P < 0.05$, and $**P < 0.0001$. (F) Time course of OFP/GFP ratios of isolated islets stimulated with various levels of glucose. Glucose levels were increased in a stepwise manner from 2.8 to 25 mM (n = 8). (G) Time course of the fluorescence emission ratio (OFP/GFP) of single cells isolated from islets expressing GO-ATeam1. The OFP/GFP ratio was monitored when glucose in the medium was increased from 2.8 to 25 mM, followed by 5 μg/mL oligomycin A addition (n = 11). (H, I) Time course of the fluorescence emission ratio (OFP/GFP) of isolated islets expressing GO-ATeam biosensors in the mitochondrial matrix. OFP/GFP ratios of mitGO-ATeam1 (H) or mitGO-ATeam3 (I) were monitored (n = 7 and 4, respectively).

FIGURE 3. Cytosolic ATP level responds more rapidly to an increase than to a decrease in glucose concentration in the medium. (A) Dynamics of the OFP/GFP ratio in isolated islets expressing GO-ATeam1 in response to alternating glucose concentrations between 2.8 and 25 mM in the medium (n = 9). (B) The average rates of change of OFP/GFP ratios upon glucose increase or decrease. The values are calculated from experiments as in (A). (C) Times required for the OFP/GFP ratio to reach 50% of the maximum value after changes in glucose concentration. The values are calculated from experiments as in (A). Error bars indicate the standard deviation (SD) and asterisks indicate significant differences. $P < 0.0001$

FIGURE 4. Both iodoacetate and oligomycin A rapidly lower $[ATP]_c$ in pancreatic islets. (A) Time course of $[ATP]_c$ in a single islet treated with 1 mM iodoacetate (n = 5). (B) Time course of $[ATP]_c$ in a single islet treated with 5 μg/mL oligomycin A (n = 5). Islets were incubated in KRH medium containing 25 mM glucose.

FIGURE 5. The increase in $[Ca^{2+}]_c$ follows that of $[ATP]_c$ in glucose-stimulated isolated islets. (A) Co-imaging of $[ATP]_c$ and $[Ca^{2+}]_c$ in single isolated glucose-stimulated islets using GO-ATeam1 and fura-2. Glucose in the medium was increased from 2.8 to 25 mM. Pseudocolored ratiometic images of GO-ATeam1 (OFP/GFP ratio, referred to as ATP) and fura-2 (340ex/380ex ratio, referred to as Ca^{2+}) are shown. The italicized letters correspond to those in B. (B) Representative time courses of $[ATP]_c$ and $[Ca^{2+}]_c$ in glucose-stimulated islets (n = 19). $[ATP]_c$ and $[Ca^{2+}]_c$ within the region of interest (white circular area) of the islet represented in A are shown. (C, D) Representative time courses of $[ATP]_c$ and $[Ca^{2+}]_c$ in glucose- (C) or tolbutamide- (D) stimulated islets pretreated with 1 mM iodoacetate. (n = 6 for both (C) and (D), respectively). (E, F) Representative time courses of $[ATP]_c$ and $[Ca^{2+}]_c$ in glucose- (E) or tolbutamide- (F) stimulated islets pretreated with 1 μg/mL oligomycin A (n = 6 for both (E) and (F), respectively). The black line represents $[ATP]_c$ and the red line represents $[Ca^{2+}]_c$.

FIGURE 6. Methyl pyruvate induces increases of intracellular ATP levels prior to Ca^{2+} influx. $[ATP]_c$, $[ATP]_m$, and $[Ca^{2+}]_c$, in single isolated islets stimulated with methyl pyruvate (MP). Islets were incubated in KRH medium without glucose for 40 minutes. (A) Representative time course of $[ATP]_m$ and $[Ca^{2+}]_c$ in single isolated islets stimulated with 20

mM MP (n = 5). (B) Representative time course of $[ATP]_c$ and $[Ca^{2+}]_c$ in single isolated islets stimulated with 20 mM MP (n = 7). (C) Representative time courses of $[ATP]_c$ and $[Ca^{2+}]_c$ in single isolated islets stimulated with 1 μg/mL oligomycin A and 20 mM MP (n = 6). The black line represents $[ATP]_m$ (A) or $[ATP]_c$ (B and C) and the red line represents $[Ca^{2+}]_c$.

FIGURE 7. Treatment with both leucine and glutamine leads to increases in intracellular ATP levels prior to Ca^{2+} influx. $[ATP]_c$, $[ATP]_m$, and $[Ca^{2+}]_c$ were monitored in single isolated islets treated with leucine and/or glutamine. Islets were incubated in KRH medium containing 2.8 mM glucose. (A, B) Dynamics of intracellular ATP and Ca^{2+} levels in leucine-stimulated single islets. $[ATP]_m$ (A) and $[ATP]_c$ (B) were monitored along with $[Ca^{2+}]_c$ in single isolated islets treated with 10 mM leucine (Leu) (n = 5 and 4, respectively). (C, D) Dynamics of intracellular ATP and Ca^{2+} levels in glutamine-stimulated single islets. $[ATP]_m$ (C) and $[ATP]_c$ (D) were monitored along with $[Ca^{2+}]_c$ in single isolated islets treated with 10 mM glutamine (Gln) (n = 3 and 5, respectively). (E, F) Dynamics of intracellular ATP and Ca^{2+} levels in leucine/glutamine-stimulated single islets. $[ATP]_m$ (E) and $[ATP]_c$ (F) were monitored along with $[Ca^{2+}]_c$ in single isolated islets treated with 10 mM leucine (Leu) in the presence of 10 mM glutamine (Gln) (n = 5 for both (E) and (F), respectively). (G) Representative time courses of $[ATP]_c$ and $[Ca^{2+}]_c$ in single isolated islets stimulated with 1 μg/mL oligomycin A and 10 mM leucine in the presence of 10 mM glutamine (n = 6). Islets were pretreated with glutamine for 20 minutes (E-G) before initiating the imaging experiments. The black line represents $[ATP]_m$ (A, C, and E) or $[ATP]_c$ (B , D, F and G), and the red line represents $[Ca^{2+}]_c$.

FIGURE 8. Correlation between $[ATP]_c$ and $[Ca^{2+}]_c$ when $[Ca^{2+}]_c$ was oscillated under high-glucose conditions. (A) Representative time courses of $[ATP]_c$ and $[Ca^{2+}]_c$ in glucose-stimulated islets showing oscillations in $[Ca^{2+}]_c$ (n = 15). Data for the four plots shown in this figure were from different islets. Islets were stimulated by increasing the glucose concentrations in the medium from 2.8 to 25 mM. (B) Cross-correlation analysis of the dynamics of $[ATP]_c$ and $[Ca^{2+}]_c$. Cross-correlation analysis was performed between the dynamics of $[ATP]_c$ and $[Ca^{2+}]_c$ in the rectangle shown in A. The trace shows the one-dimensional cross-correlation, with the time difference (t) of the correlation on the x-axis and the numerically expressed cross-correlation amplitude on the y-axis. (C) Dynamics of $[ATP]_c$ during Ca^{2+} oscillations induced by high glucose levels and further augmentation of glucose in the medium. $[ATP]_c$ and $[Ca^{2+}]_c$ in single islets were monitored after stimulation with

25 mM and further with 42 mM glucose (n = 6). (D) Representative time course of $[ATP]_c$ and $[Ca^{2+}]_c$ in an islet stimulated with various levels of glucose. Glucose levels were increased in a stepwise manner from 2.8 to 25 mM (n = 12). The black line represents $[ATP]_c$ and the red line represents $[Ca^{2+}]_c$.

FIGURE 9. Dynamics of $[ATP]_c$ and $[Ca^{2+}]_c$ when glucose-induced $[Ca^{2+}]_c$ oscillations were stopped. (A) Representative time course of $[ATP]_c$ and $[Ca^{2+}]_c$ in islets showing $[Ca^{2+}]_c$ oscillations, treated with 4 μM CCCP (n = 5). Islets were incubated in KRH medium containing 25 mM glucose. (B) Representative time course of $[ATP]_c$ and $[Ca^{2+}]_c$ in islets upon reduction of the glucose concentration (n = 5). The black line represents $[ATP]_c$ and the red line represents $[Ca^{2+}]_c$.

FIGURE 10. Dependence of glucose-induced intracellular ATP elevation on intracellular Ca^{2+}. (A-D) The effect of Ca^{2+} depletion from the medium. $[ATP]_m$ (A, B) or $[ATP]_c$ (C, D) was monitored in isolated islets when the glucose level was elevated from 2.8 to 20 mM (n = 5 for both (A) and (C), n = 6 for both (B) and (D), respectively). Islets were pretreated with Ca^{2+}-depleted KRH medium (A, C) or normal Ca^{2+}-containing KRH medium (B, D) for 40 minutes. (E, F) The effect of intracellular Ca^{2+} depletion. $[ATP]_m$ (E) or $[ATP]_c$ (F) were monitored in isolated islets when the glucose level was elevated from 2.8 to 20 mM (n = 5 for both (E) and (F), respectively). Islets were pretreated with 5 μM 1,2-bis(o-aminophenoxy)ethane-N,N,N′,N′-tetraacetic acid (BAPTA)-AM (BAPTA) for 20 minutes. (G) Depletion of intracellular Ca^{2+} decreases basal $[ATP]_m$. Time course of $[ATP]_m$ in islets treated with 5 μM BAPTA-AM (BAPTA). Islets were incubated in KRH medium containing 2.8 mM glucose (n = 5).

Figure 1

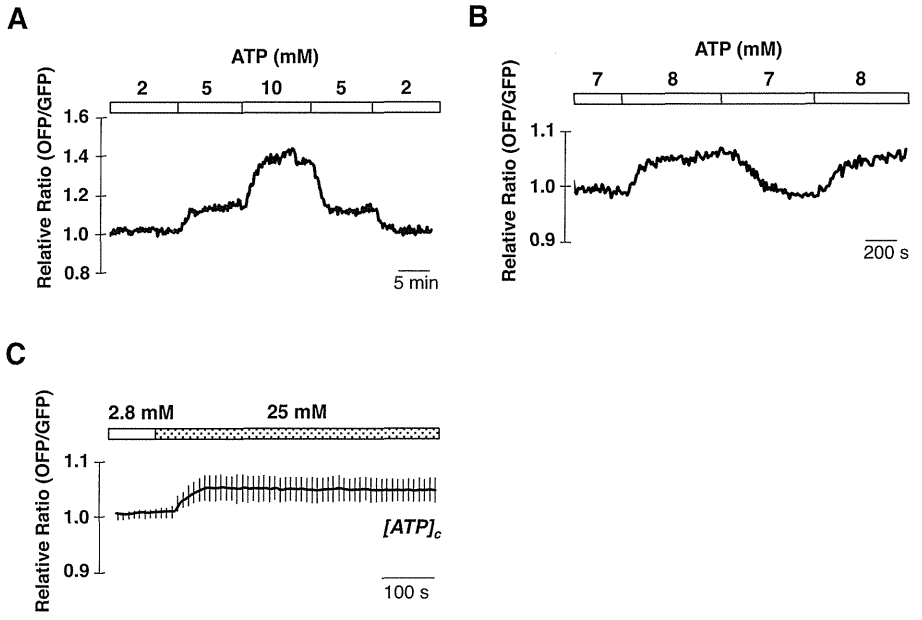

Figure 2

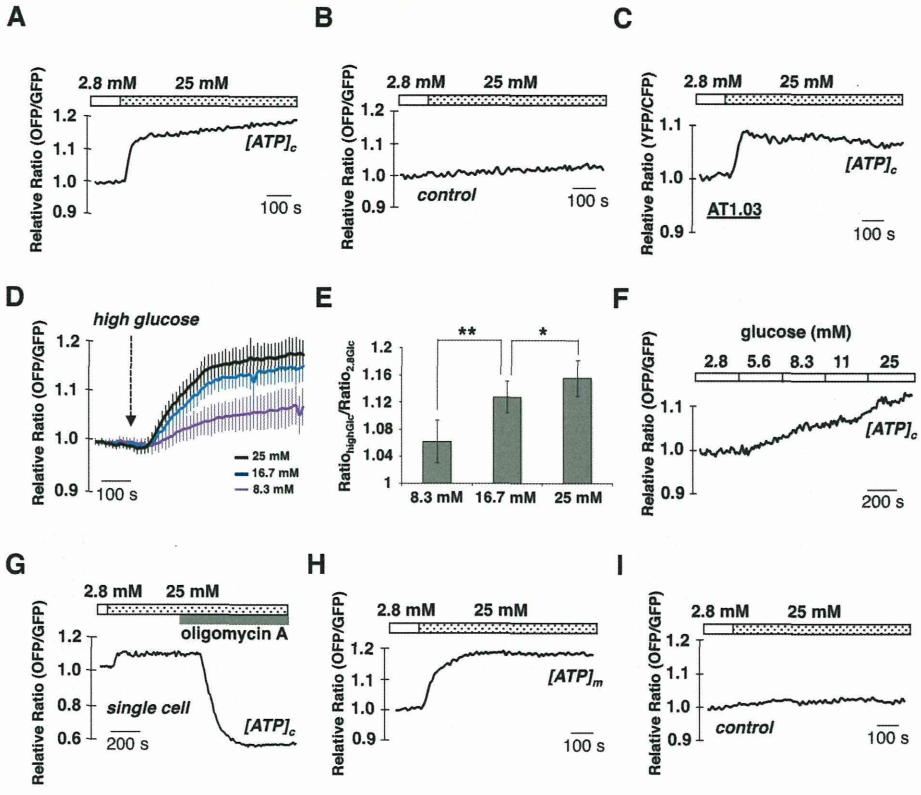
A
2.8 mM
25 mM
Relative Ratio (OFP/GFP)
[ATP]c
100 s
B
control
C
Relative Ratio (YFP/CFP)
AT1.03
D
high glucose
25 mM
16.7 mM
8.3 mM
E
8.3 mM
16.7 mM
25 mM
F
glucose (mM)
2.8
5.6
8.3
11
25
200 s
G
oligomycin A
single cell
H
[ATP]m
I

Figure 3

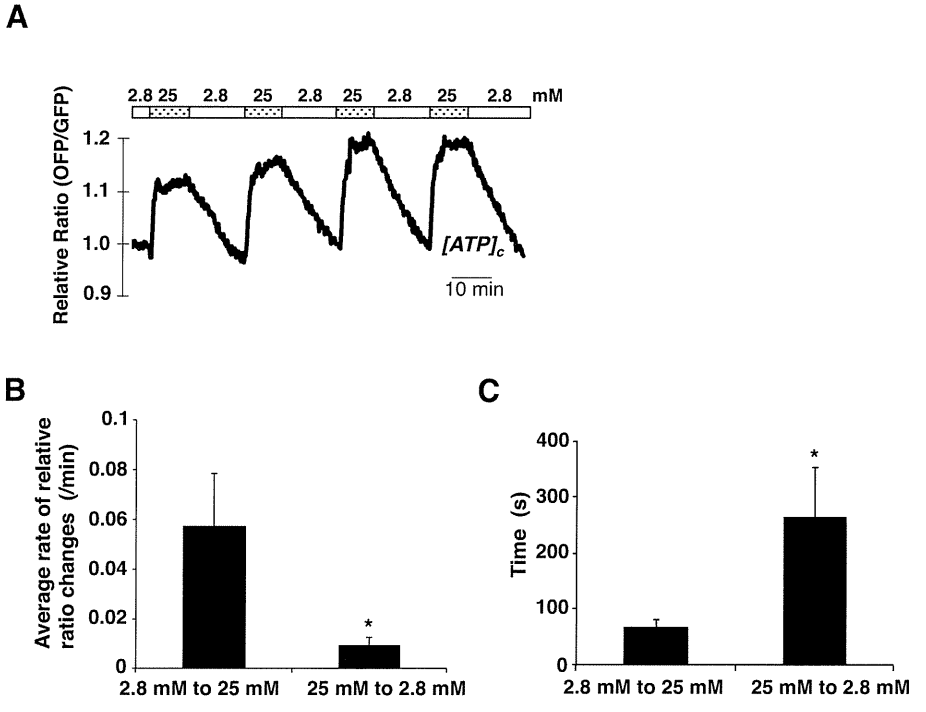
A
2.8 25 2.8 25 2.8 25 2.8 25 2.8 mM
Relative Ratio (OFP/GFP)
1.2
1.1
1.0
0.9
[ATP]c
10 min
B
Average rate of relative ratio changes (/min)
0.1
0.08
0.06
0.04
0.02
0
*
2.8 mM to 25 mM
25 mM to 2.8 mM
C
Time (s)
400
300
200
100
0
*
2.8 mM to 25 mM
25 mM to 2.8 mM

Figure 4

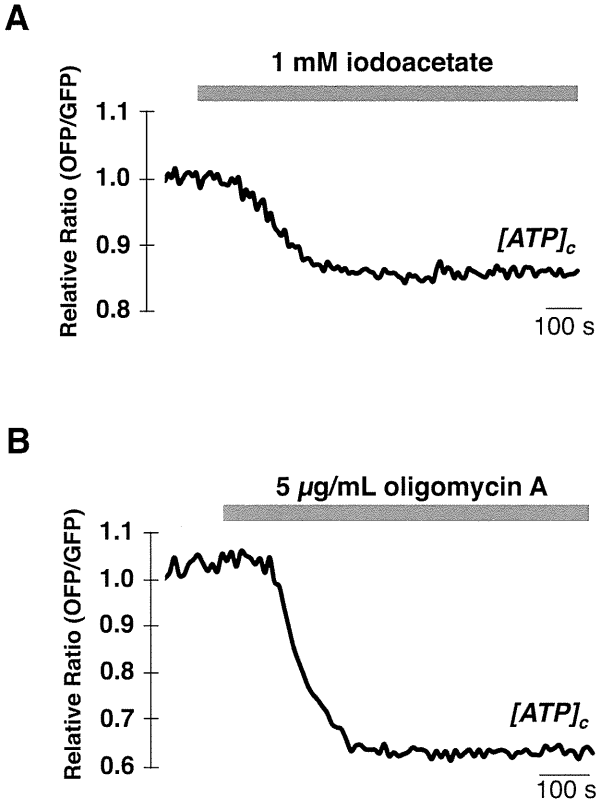
A
1 mM iodoacetate
Relative Ratio (OFP/GFP)
1.1
1.0
0.9
0.8
[ATP]c
100 s
B
5 μg/mL oligomycin A
Relative Ratio (OFP/GFP)
1.1
1.0
0.9
0.8
0.7
0.6
[ATP]c
100 s

Figure 5

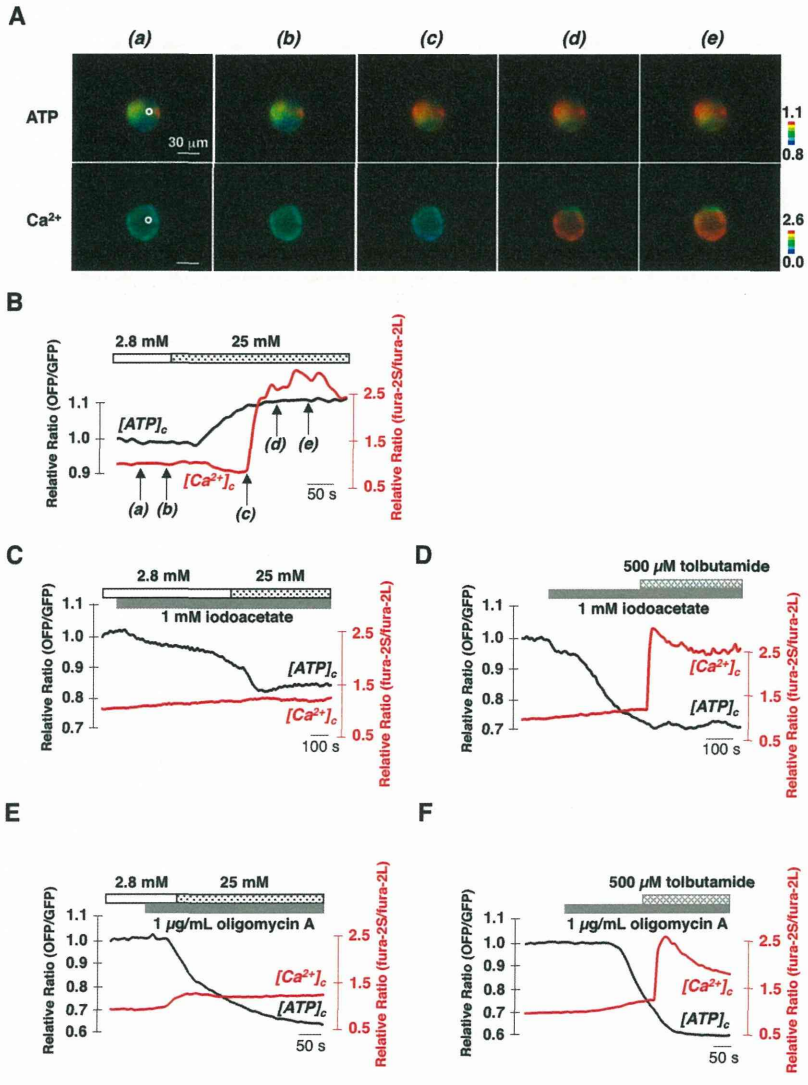
A
(a)
(b)
(c)
(d)
(e)
ATP
30 μm
1.1
0.8
Ca2+
2.6
0.0
B
2.8 mM
25 mM
Relative Ratio (OFP/GFP)
[ATP]c
[Ca2+]c
(a) (b)
(c)
(d) (e)
50 s
Relative Ratio (fura-2S/fura-2L)
C
2.8 mM
25 mM
1 mM iodoacetate
100 s
D
500 μM tolbutamide
1 mM iodoacetate
100 s
E
2.8 mM
25 mM
1 μg/mL oligomycin A
50 s
F
500 μM tolbutamide
1 μg/mL oligomycin A
50 s

Figure 6

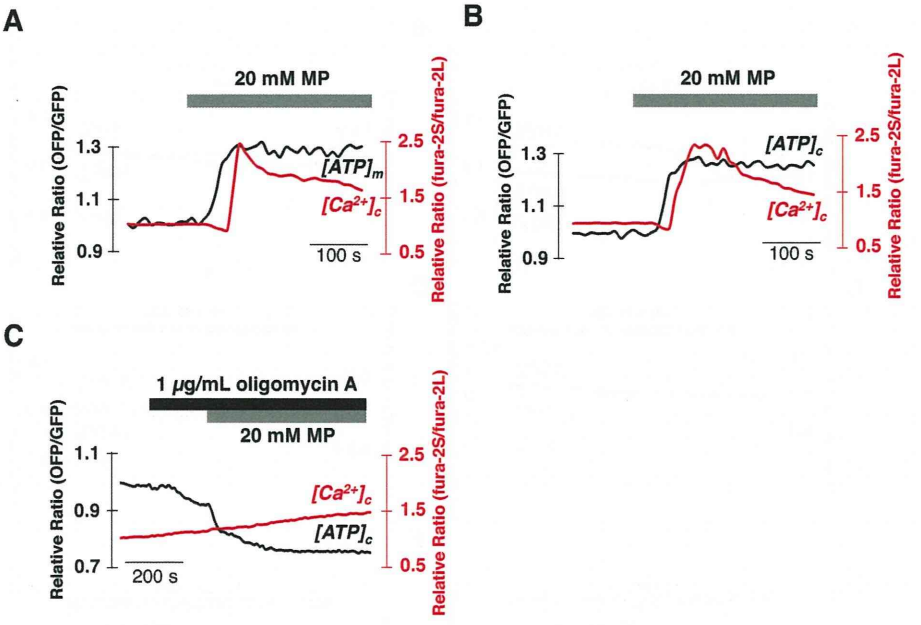
A
20 mM MP
Relative Ratio (OFP/GFP)
1.3
1.1
0.9
[ATP]m
[Ca2+]c
100 s
2.5
1.5
0.5
Relative Ratio (fura-2S/fura-2L)
B
20 mM MP
Relative Ratio (OFP/GFP)
1.3
1.1
0.9
[ATP]c
[Ca2+]c
100 s
2.5
1.5
0.5
Relative Ratio (fura-2S/fura-2L)
C
1 µg/mL oligomycin A
20 mM MP
Relative Ratio (OFP/GFP)
1.1
0.9
0.7
[Ca2+]c
[ATP]c
200 s
2.5
1.5
0.5
Relative Ratio (fura-2S/fura-2L)

Figure 7

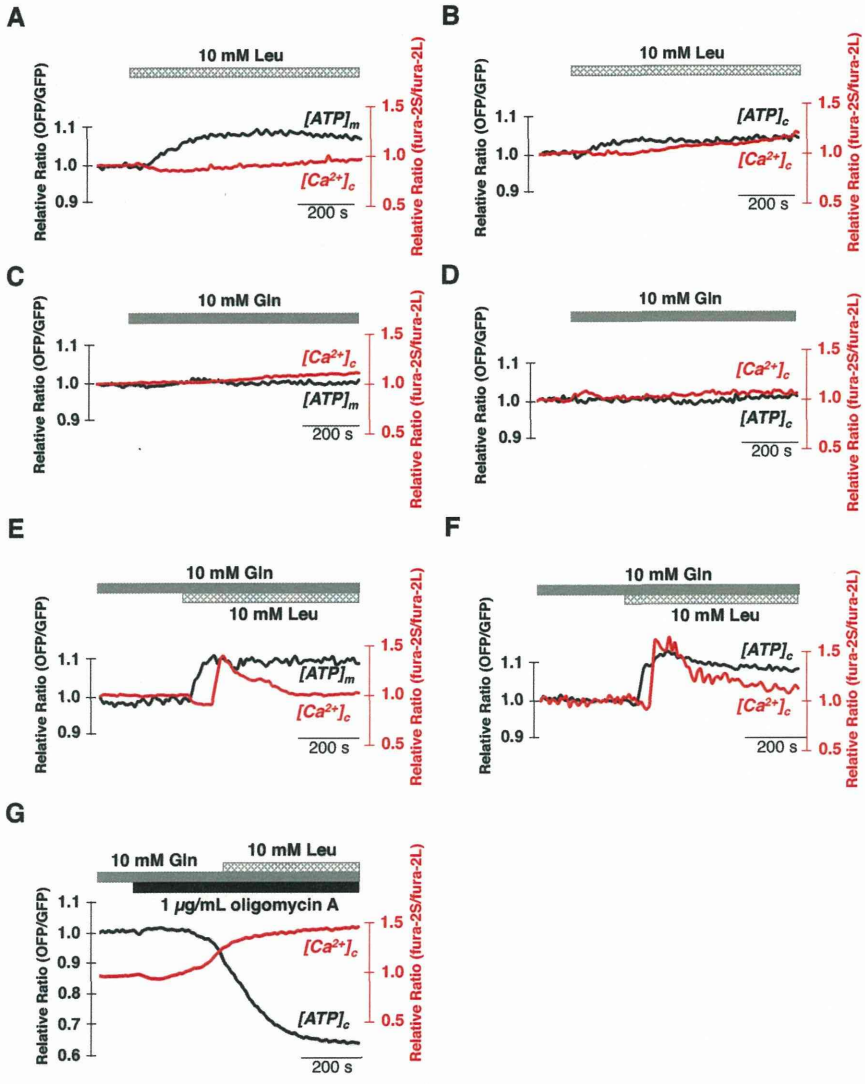
A
10 mM Leu
[ATP]m
[Ca2+]c
200 s
Relative Ratio (OFP/GFP)
Relative Ratio (fura-2S/fura-2L)
B
10 mM Leu
[ATP]c
[Ca2+]c
200 s
C
10 mM Gln
[Ca2+]c
[ATP]m
200 s
D
10 mM Gln
[Ca2+]c
[ATP]c
200 s
E
10 mM Gln
10 mM Leu
[ATP]m
[Ca2+]c
200 s
F
10 mM Gln
10 mM Leu
[ATP]c
[Ca2+]c
200 s
G
10 mM Gln
10 mM Leu
1 µg/mL oligomycin A
[Ca2+]c
[ATP]c
200 s

Figure 8

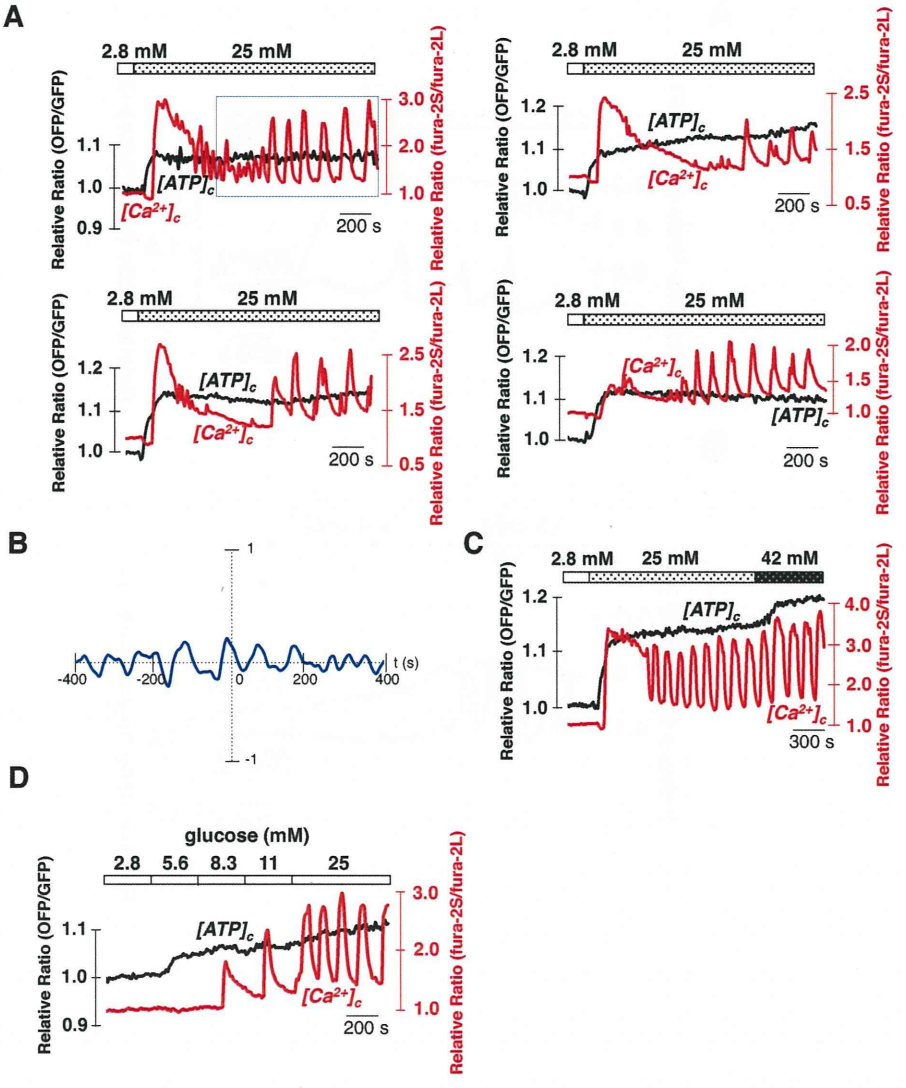
A
2.8 mM
25 mM
Relative Ratio (OFP/GFP)
Relative Ratio (fura-2S/fura-2L)
[ATP]c
[Ca2+]c
200 s
B
t (s)
-400
-200
0
200
400
1
-1
C
42 mM
300 s
D
glucose (mM)
2.8
5.6
8.3
11
25

Figure 9

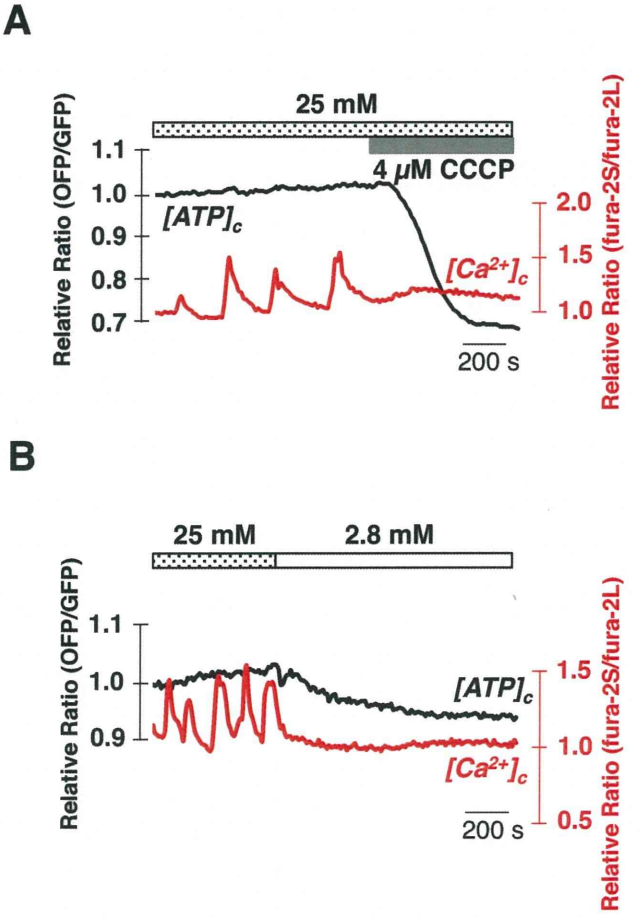
A
25 mM
4 μM CCCP
[ATP]c
[Ca2+]c
Relative Ratio (OFP/GFP)
1.1
1.0
0.9
0.8
0.7
2.0
1.5
1.0
200 s
Relative Ratio (fura-2S/fura-2L)
B
25 mM
2.8 mM
Relative Ratio (OFP/GFP)
1.1
1.0
0.9
[ATP]c
[Ca2+]c
1.5
1.0
0.5
200 s
Relative Ratio (fura-2S/fura-2L)

Figure 10

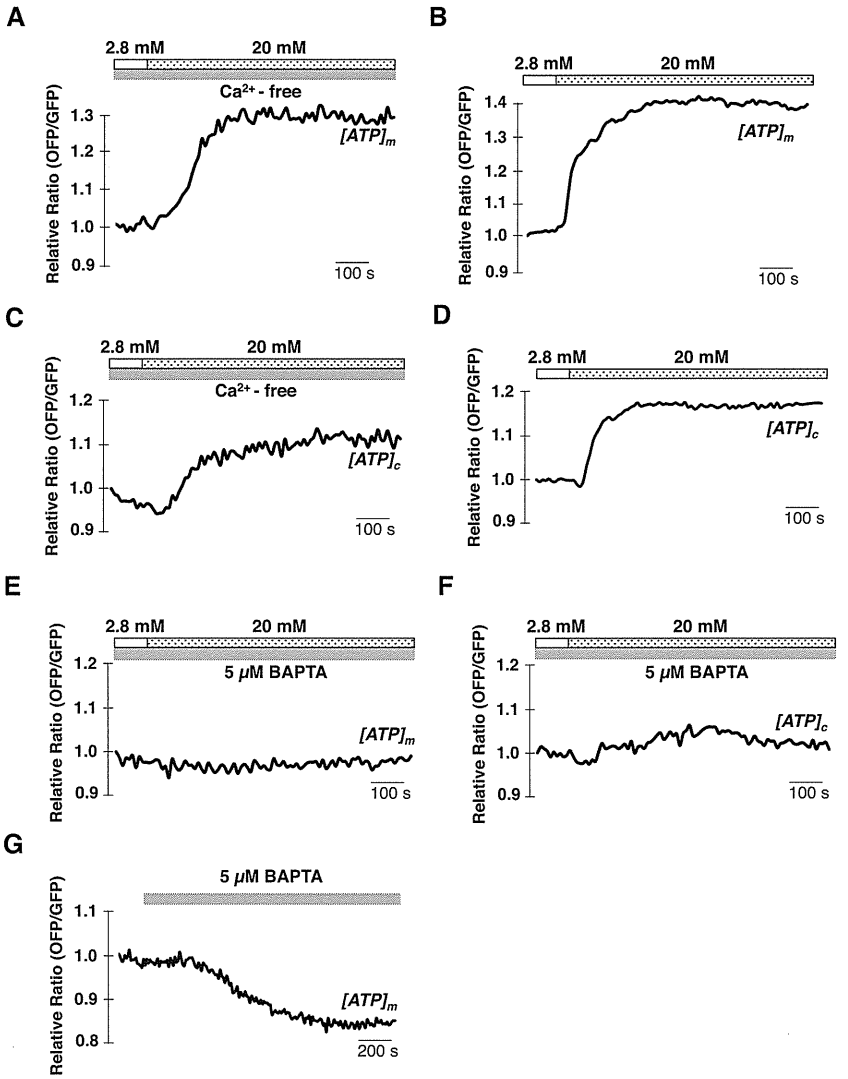
A
2.8 mM
20 mM
Ca2+ - free
[ATP]m
Relative Ratio (OFP/GFP)
1.3
1.2
1.1
1.0
0.9
100 s
B
2.8 mM
20 mM
[ATP]m
Relative Ratio (OFP/GFP)
1.4
1.3
1.2
1.1
1.0
0.9
100 s
C
2.8 mM
20 mM
Ca2+ - free
[ATP]c
Relative Ratio (OFP/GFP)
1.2
1.1
1.0
0.9
100 s
D
2.8 mM
20 mM
[ATP]c
Relative Ratio (OFP/GFP)
1.2
1.1
1.0
0.9
100 s
E
2.8 mM
20 mM
5 μM BAPTA
[ATP]m
Relative Ratio (OFP/GFP)
1.2
1.1
1.0
0.9
100 s
F
2.8 mM
20 mM
5 μM BAPTA
[ATP]c
Relative Ratio (OFP/GFP)
1.2
1.1
1.0
0.9
100 s
G
5 μM BAPTA
[ATP]m
Relative Ratio (OFP/GFP)
1.1
1.0
0.9
0.8
200 s